Phylogeny of *Weinmannia* (Cunoniaceae) reveals the Contribution of the Southern Extratropics to Tropical Andean Biodiversity.

Ricardo A. Segovia*[1,2], Eduardo Aguirre-Mazzi*[3,4], Christine E. Edwards[5], Alexander G. Linan[6], Alfredo Fuentes[4,7], Andrea Chaspuengal[8], Kyle G. Dexter[9,10], Francisco Fajardo[11], William Farfan-Rios[12,13], Nora H. Oleas[8], Juan C. Penagos Zuluaga[14], J. Sebastián Tello[4]

[1] *Departamento de Botánica, Universidad de Concepción, Chile;* [2] *Institute of Ecology and Biodiversity (ieb-chile.cl);* [3] *Department of Biology, Washington University in St. Louis, St. Louis, MO, United States;* [4] *Latin America Department, Missouri Botanical Garden, St. Louis, MO, United States;* [5] *Center for Conservation and Sustainable Development, Missouri Botanical Garden, St. Louis, MO, United States:* [6] *Africa and Madagascar Program, Missouri Botanical Garden, St. Louis, MO, United States;* [7] *Herbario Nacional de Bolivia, Instituto de Ecología, Carrera de Biología, Universidad Mayor de San Andrés, La Paz, Bolivia.;* [8] *Centro de Investigación de la Biodiversidad y Cambio Climático (BioCamb) y Facultad de Ciencias del Medio Ambiente, Universidad Tecnológica Indoamérica, Machala y Sabanilla, Quito, Ecuador;* [9] *School of GeoSciences, University of Edinburgh;* [10] *Royal Botanic Garden Edinburgh;* [11], *14195 Berlin, Germany;* [12] *Department of Biology, Wake Forest University, Winston-Salem, NC 27106, USA.;* [13] *Andrew Sabin Center for Environment and Sustainability, Wake Forest University, Winston-Salem, NC 27106, USA.;* [14] *Research Affiliate Yale School of the Environment, Yale University. 195 Prospect Street, New Haven, CT.;* * These authors contributed equally to this work

Corresponding author; e-mail:

rsegovia@ieb-chile.cl;
christine.edwards@mobot.org

Abstract

The Andes are a relatively young mountain range with an impressive concentration of biodiversity. The biogeographic processes contributing to the hyperdiversity of the tropical Andes are still being unraveled. Novel mid- to high-elevation climates may have served as a biological corridor for the immigration of temperate-adapted lineages to lower latitudes, contributing unknown levels of diversity to this region. We tested the hypothesis that the genus *Weinmannia* corresponds to a lineage of extratropical origin that recently reached and then diversified extensively in tropical Andes. Using a 2bRAD seq approach to generate a time-calibrated phylogenetic tree for the genus, we found that the earliest diverging clades represent southern extratropical species, and a tendency for younger clades to be distributed towards northern latitudes. These results suggest a dispersal route for *Weinmannia* from the southern extratropics to the tropical Andes. As remnants of these lineages of southern origin converge with those that originated in other tropical and extratropical centers of diversification, we provide insights into the multisource origins of hyperdiversity in the modern montane forests of the tropical Andes.

Keywords: immigration, diversification, hyperdiversity, tropics, Gondwana

Introduction

The Andean region of tropical America has one of the world's highest levels of species richness (Balsev 1993), taxonomic endemism (Myers et al. 2000) and phylogenetic diversity (Tietje et al. 2023). This hyperdiversity is particularly intriguing given that the modern geomorphology of this area is no older than the late Miocene (< 11 Ma) (Gregory-Wodzicki 2000; Siravo et al. 2018). Mountain building is generally thought to have fostered high levels of diversity in a variety of ways, including the speciation of resident lineages (Rahbek et al. 2019) and the immigration of lineages pre-adapted to newly created climatic conditions (Donoghue 2008). Indeed, the Andean orogeny may have increased the rate of lineage diversification (Antonelli and Sanmartin 2011a; Hazzi et al. 2018) and may also have opened a corridor for the immigration of temperate lineages into the lower latitudes of tropical America (Graham 1973; Segovia and Armesto 2015). Comprehensive evolutionary evidence is still being gathered to identify areas of lineage origin and thus unravel the relative influence of these biogeographic processes in shaping the modern pattern of hyperdiversity in the Andes.

Phylogenetic evidence shows faster-than-expected rates of diversification for a number of potentially resident plant clades in synchrony with the Andean uplift since the early Miocene (e.g., Luebert and Weigend 2014; Givnish et al. 2014; Schwery et al. 2015; Spriggs et al. 2015; Perez-Escobar et al. 2017, 2022, Dellinger et al. 2024). Moreover, a growing body of phylogenetic evidence shows immigration processes from both the northern and southern extratropics into the tropical Andes. Many lineages have immigrated from the northern extratropics, including examples such as *Viburnum* (Winkworth and Donoghue 2005), *Lupinus* (Hughes and Eastwood 2006), and *Passiflora* section *Decaloba* (Acha et al. 2021). Conversely, there is less evidence for lineages that likely arrived in the tropical Andes from the southern extratropics, although notable examples include Alstroemeriaceae (Chacón et al. 2012), *Podocarpus* (Quiroga et al. 2016), *Gunnera* (Bacon et

al. 2018), and Loranthaceae (Liu et al. 2018). However, most of what we know about these biogeographic scenarios for the origin of the plant diversity in the tropical Andes is biased toward clades inhabiting open biomes at high-elevations. Evidence regarding the origin and direction of dispersal routes of the clades that comprise montane forests at intermediate elevations still remains scarce, and represents a significant gap in our understanding of plant diversity and evolution in one the most species-rich region on the planet.

The idea that lineages from the relatively species-poor extratropics could contribute to the modern hyperdiversity of the tropical Andes is counterintuitive. Traditionally, the highest levels of species richness are thought to be associated with "centers of diversification" (Willis 1922), or areas where a particular lineage originated (Wiens and Donoghue 2004). In addition, there is strong evidence that the American tropics have historically acted as a "species pump" for global plant diversity (Antonelli et al. 2015). However, the immigration from multiple zones, including the extratropics, into tropical Andean forests has also been documented based on taxonomic affinities (Hooghiemstra 1984), fossil records (Graham 1995), and community phylogenetics (González-Caro et al. 2023), rather than just clade reconstructions. These multisource immigration processes, along with rapid lineage diversification, may be key to shaping the modern hyperdiversity of the tropical Andes, increasing not only taxonomic diversity but also evolutionary diversity, according to the "environmental crossroads hypothesis" (Neves et al. 2020). For example, the exceptionally high levels of different measures of phylogenetic diversity in the central and northern Andes (Tietje et al. 2023) may be due to the mixing of deeply isolated biotas with different evolutionary histories (e.g., remnants of paleobiotas from Holartic, Austral and Neotropical floristic realms).

Here we investigate the biogeography of *Weinmannia* L. (*sensu* Pillon et al. 2021), formerly *Weinmannia* sect. *Weinmannia* L. (Bradford, 1998), a genus of trees and shrubs that are important components of ecosystem

functioning of Andean forests owing to their abundance and diversity. Typically considered a southern hemisphere taxon, *Weinmannia* consists of two species occurring in the Mascarenes and over 80 species in the Americas (Bradford 1998, 2002; Ulloa-Ulloa et al. 2017; Pillon et al. 2021). The higher diversity of *Weinmannia* occurs at mid- to high- elevations in the tropical Andes, where it exhibits weak species boundaries and overlapping morphologies due to either recent divergence or hybridization (Bradford 1998, 2002). In addition, several species occur in the Pantepui region, and the mountain peaks of Central America and the Caribbean Islands. One species is endemic to the subtropical forests of eastern Brazil (i.e., Mata Atlantica), and another species occurs in the temperate forests of southern South America (Chile and Argentina) (Gentry 1982, 1995). Previous phylogenies placed the only southern extratropical species (*Weinmannia trichosperma* Cav.) at the base of the *Weinmannia* clade (Bradford 1998, 2002), sparking the hypothesis that *Weinmannia* immigrated recently into the tropical Andes from the southern extratropics (Bradford et al. 2004; Pennington and Dick 2004). However, these analyses sampled only a small proportion of the species in the genus and employed only a small number of plastid and/or nuclear regions (Bradford 2002; Pillon et al. 2021), preventing hypothesis testing about the origin and dispersal of *Weinmannia* across the Andes.

To examine the hypothesis of a southern extratropical origin for *Weinmannia* and a recent immigration into the tropical Andes, we constructed a new NGS phylogeny with a comprehensive taxon sampling. First, we tested the prediction that if the genus *Weinmannia* originated in the southern extratropics, then *W. trichosperma* from the temperate forests of southern South America should be placed as a sister group to all other *Weinmannia* species of the Americas. Second, we tested the prediction that if the modern distribution of *Weinmannia* is a consequence of dispersal from the southern extratropics into the tropical Andes, then the ages of nodes in the phylogeny should show a negative relationship with the reconstructed

latitude of the nodes. In other words, the phylogeny should show a pattern in which younger clades occupy successively more northern latitudes.

Materials & Methods

Sampling and genomic DNA extraction. We collected 896 samples of *Weinmannia* from across South America, including the southern Andes (Chile), the central Andes (Bolivia and Peru), and the northern Andes (Ecuador and Colombia). We also included four samples from the Mascarene Islands. For each sample, we preserved leaf tissue in silica and collected an herbarium voucher specimen. In addition, we included five specimens from three species of *Pterophylla* (*sensu* Pillon et al. 2021) as outgroups.

To extract DNA, silica-dried tissues were first ground and then cleaned using up to three sorbitol washes following Inglis et al. (2018) to remove mucilage and other secondary compounds. Genomic DNA was extracted using a modified CTAB extraction protocol for plants (based on Doyle and Doyle et al. 1987), with additional ethanol washes of precipitated DNA. Finally, following extraction, DNA was purified using KAPA pure Beads (KAPA Biosystems) following manufacturer protocols. DNA concentrations were quantified using a Qubit™ fluorometer (ThermoFisher).

Sequencing. RAD-seq libraries were prepared using a 2b-RAD approach (Wang et al. 2012) and previously published protocols for the method (Linan et al. 2021b; Mashburn et al. 2023). We digested approximately 500 ng of purified genomic DNA of each sample, using the type-IIB restriction enzyme BcgI (New England Biolabs), which produced 36 bp DNA fragments from across the nuclear genome of each specimen. To ensure adequate sequence coverage per locus, 5′-NNG-3’ selective adapters were used to decrease the number of sequenced loci, as described by Wang et al. (2012). 96 samples were pooled per plate through the use of dual index barcodes, whereby the first barcode applied across columns allow pooling of the 8 rows. Each of

these pools was amplified with incorporating the second barcode index (one of 8 unique 6 bp Illumina TruSeq barcodes) and an Illumina primer using high fidelity Phusion PCR mix (New England Biolabs) for 14 cycles of PCR amplification. The resulting amplicons were purified using 2% Agarose gel purification with a MinElute gel purification kit (Qiagen). The purified ligation pools were mixed at equimolar proportions after measuring concentrations in the Qubit fluorometer (Qiagen). The final library obtained was sequenced on an Illumina HiSeq 4000, generating 50 bp single end reads at the NUSeq Core facility of Northwestern University.

RAD locus assembly. The quality of raw reads was checked using FastQC (Andrews, 2010). Sequences were demultiplexed and trimmed to remove barcodes and Illumina adaptors using the trim2bRAD_2barcodes_noAdap.pl script available in *2bRAD-Edwards-Lab* git repository (https://github.com/Kenizzer/2bRAD-Edwards-Lab). Trimmed reads were assembled *de novo* using the ipyrad v. 0.9.90 pipeline (Eaton 2020). To determine the optimum clustering threshold, we iterated clustering threshold within samples (CTWS) and among samples (CTAS) using every combination of values of 0.86, 0.89, 0.92, and 0.94. The resulting matrices were compared for cluster depth, heterozygosity, the amount of putatively paralogous loci, and the number of SNPs to identify parameters that could lead to assembly errors (Paris et al. 2017). Following this approach, we selected a value of 0.92 for both CTWS and CTAS. We filtered all loci including gaps and retained all loci with no more than five SNPs.

Identification of putative hybrids. To identify putative hybrid individuals that may confound phylogenetic analysis, we assessed admixture using STRUCTURE v. 2.3.4 (Pritchard et al. 2000) as implemented in ipyrad v. 0.9.90. Due to the large number of samples and putative species, we divided samples and conducted a series of analyses within two geographically structured groups (central Andes region and northern Andes region), given that interspecific gene flow is most likely to occur among geographically

proximal species. For each of these analyses, we conducted an independent assembly with the clustering threshold 0.92 removing all individuals with more than 80% missing sites, retaining loci present in at least 50% of samples, and retaining one SNP per locus. STRUCTURE analyses were run under an admixture model with a burn-in of 300,000 generations and a run length of 700,000 generations. The number of genetic clusters assessed (K) was defined according to the number of species within each sub analysis going from K=2 to 20. A total of 15 repetitions were run for each K value. The optimal *K* value was selected using the Evanno method (Earl and von Holdt 2011). We defined putative hybrids as individuals with less than 85% assignment to a single genetic cluster, adopting a slightly more conservative criterion compared to the 80% cut-off used by Lindtke et al. (2014), Owusu et al. (2015) and Linan et al (2021).

Individual-level tree inference. For phylogenetic inference, we chose 3-5 individuals with no signature of hybridization from each species. This resulted in 234 accessions, spanning 48 *Weinmannia* taxa (including 6 that are not assigned to any described species), plus 3 *Pterophylla* species as outgroups (total 51 species). This dataset includes a representative sample of the 75 (Ulloa-Ulloa et al. 2017) to 90 (Pillon et al. 2021) *Weinmannia* species estimated to occur in the Americas.

Maximum likelihood (ML) phylogenetic analysis was conducted using concatenated 36 bp fragments, including invariant sites. First, we performed preliminary analysis to explore the effect of missing data on the resulting topologies, varying the percentage of samples at which a locus must be present to be retained from 4% to 48% in increments of 4. We found optimal branching resolution and bootstrap supports when all loci were present in at least 36% (84/234) of samples. The ML phylogeny was inferred in RAxML v. 8.2.12 (Stamatakis 2014) using a rapid hill climbing algorithm and the GTRCAT approximation. Clade supports were calculated using the transfer bootstrap approach with 200 iterations (Lemoine et al. 2018).

Species-level *Weinmannia* phylogeny. To reconstruct a species-level phylogeny, the individual-level phylogeny (Supplementary Fig. 1) was used to select one representative individual from each species (defined as a reciprocally monophyletic group of individuals that had morphological distinctiveness). We choose non-admixed individuals (as indicated by STRUCTURE) with the least amount of missing data. To infer a phylogeny, we employed both a ML analysis of the concatenated loci and SVDQuartets, which is a multi-species coalescent-based approach (Chifman & Kubatko 2014). For the species-level ML analysis, we followed the same approach as described for the individual-level phylogeny. After preliminary analysis to explore the effect of missing data, we prepared a concatenated alignment of all loci present in at least 32% (16/51) of all individuals. This matrix was used to infer a phylogeny in RAxML (Stamatakis 2014). The multi-species coalescent-based phylogenetic inference was performed using a randomly selected SNP from each of the 2,879 loci used in the RAxML analysis. We inferred all 249,900 possible quartets for 51 taxa and conducted 500 bootstrap iterations. The quartet trees were joined into a super tree. Finally, we calculated bootstrap support (BS) for nodes using a transfer bootstrap approach (Lemoine et al. 2018). For visualization, the resulting trees were rooted on the branch containing all *Pterophylla* specimens.

Time-calibrated phylogeny. Bayesian inference of divergence times may not always be suitable for RAD-Seq data due to statistical and computational challenges (*e.g.* Donoghue et al. 2022). We thus inferred divergence times using treePL (Smith and O'Meara 2012), which relies on optimized branch length information for estimating divergence times under phylogenetic penalized likelihood. Divergence times were estimated following Maurin (2008) using our maximum likelihood (ML) tree. Optimal parameters for treePL were estimated by running the program with the prime option, with the smoothing parameter estimated with a cross-validation analysis. Confidence intervals of divergence times were estimated with a bootstrap analysis in RAxML using the option -g and the ML tree to constrain the

topology, and the option -k to optimize branch lengths in each of 200 bootstrap iterations performed. These bootstrap trees were time calibrated using the same treePL parameter as for the ML tree. A consensus tree was built in TreeAnotator v. 2.5.2 (Drummond and Rambaut 2007) using the time-calibrated ML tree and the branch-length-bootstrap trees with 0% burn-in, median heights with the target tree option.

Three calibration points were defined for divergence time estimation. The first was a *Weinmannia* pollen fossil collected from the northern Andes of Colombia dated to ~3 Ma (Hooghiemstra 1989; Van Der Hammen et al. 1973). This age was defined as the minimum age for the most recent common ancestor of the clade that encompassed all specimens collected in the Northern Andes. The second point was derived from a fossil pollen record of *Weinmannia potosina* from Potosí, Bolivia (Berry 1917; Graham et al. 2001). Using the age of this record, we established 13.8 Ma as the minimum age for the most recent common ancestor (MRCA) of the clade containing all Central and Northern Andean *Weinmannia* species. The upper limit for this point was set at 33 Ma, aligning with the proposed beginning of the Oligocene epoch (Walker et al. 2012), which is close to previous estimates for the stem node of *Weinmannia* at 32.3 Ma (Pillon et al. 2021). Additionally, we used the 95% credibility interval from Pillon et al. (2021) to estimate the divergence time between *Weinmannia* and its sister genus *Pterophylla*, setting this calibration point with a uniform distribution, with a minimum age of 29.99 Ma and a maximum age of 34.4 Ma (Pillon et al. 2021).

Testing of our biogeographic hypotheses. To test our hypothesis, that *Weinmannia* migrated from south to north, we perform ancestral reconstruction of latitude using our time-calibrated species-level phylogeny. We determined the minimum and mean latitude of each species in our phylogeny based on our geo-referenced occurrence data derived from herbarium specimens. We conducted ancestral reconstruction of (minimum

and mean) latitude using a Brownian Motion model on a pruned phylogeny without outgroups that included 48 *Weinmannia* species using the 'ace' function in the phytools v. 2.1 R package (Revell, 2012). We report only the minimum latitude results here, as the mean latitude estimates were less reliable due to insufficient records per species.

Using data from the ancestral reconstruction, we modeled the age of hypothetical ancestors (nodes) as a function of their minimum latitude. For this purpose, we employed two distinct statistical approaches: a Bayesian approach and a frequentist approach based on a Null-Hypothesis Significance Test and non-parametric bootstrap.

Bayesian regression analysis. We developed a hierarchical Bayesian regression that evaluated correlation structures derived from nesting patterns between nodes in the phylogeny, allowing us to account for the underlying evolutionary relationship between our observations (i.e., node age and reconstructed latitude). The model was built in Stan v. 2.18.2 (Carpenter et al. 2017), which uses Hamiltonian MCMC to draw posterior samples and it was implemented in R with the rstan package v. 2.26.23 (Stan Development Team 2023). Full stan code can be found in Supplementary Materials 1. First, the model was built by defining a linear predictor function as follows:

$$\mu_{n\,=} = \alpha_{int} + \beta * X_n + \theta_n \qquad (1)$$

where μ_n is the linear predictor representing the expected value of node age Y_n for each observation at each node n, α_{int} is the intercept, X_n is the estimated ancestral latitude of node n, β is the estimated slope coefficient representing the change in the expected value of Y for a one-unit change in X, and θ_n is the random effect parameter for each node n capturing unexplained variation due to unobserved factors not accounted for by X. Random effects were drawn from a multivariate normal distribution according to the following function:

$$\theta n \sim multinormal(0_N, \Sigma) \qquad (2)$$

where 0_N is the mean vector, defined as a zero vector of length N (representing the number of nodes), and Σ is a covariance matrix, in this case, given by the phylogenetic covariance matrix. We created this covariance matrix using the makeL1 function from the RRphylo package in R (Castiglione et al. 2018). This function constructs an NxN matrix of branch lengths for all root-to-node paths given a phylogeny, capturing the hierarchical relationships among each pair of nodes. Consequently, the random effects are modeled to reflect correlations produced by the shared evolutionary history among nodes. This approach allows for a more realistic representation of the data's underlying dependencies.

Using the linear predictor function and incorporating random effects (equations 1 and 2), node age Y_n was modelled using a likelihood function assuming a normal distribution of errors and identity link-function as follows:

$$Yn \sim normal(\mu_n, \varepsilon_n) \qquad (3)$$

where ε_n is the residual standard deviation capturing the unexplained variation in Y after accounting for the independent variable (X) and random effects (θ). The model was fitted to the data by running 4 independent Markov Chain Monte Carlo (MCMC) chains, each for 3 million iterations. For computational efficiency, the chains were thinned every 10 iterations, resulting in a total of 300,000 MCMC samples per chain. Of these, we discarded the first 50,000 samples as burn-in. The parameter max_treedepth was set to a minimum of 10 to handle divergent transitions during MCMC sampling.

Model adequacy was evaluated with a posterior predictive check by generating predicted values of node age from the posterior distribution using the calculated μ_n and ε_n and comparing them with the observed data (Fig. 3B and Supplementary Fig. 5B). The performance and reliability of the MCMC was evaluated with the Gelman-Rubin statistics (Rhat), effective Sample Size, and autocorrelation analysis, among others (Supplementary Materials 2

and 3: MCMC diagnostics for ML phylogeny and SVDQ respectively). Results of Bayesian regression were used to test the hypothesis that older ancestors are associated with more southern latitudes leading to a negative slope ($\beta<0$, given the predominantly negative nature of latitude values), and to assess whether we can reject the null hypothesis ($\beta\approx0$, implying no clear relationship). For this, we obtained the posterior probability distribution of the latitude slope parameter (β), from which we extracted a 95% credibility interval and determined the maximum *a posteriori* estimate. The credibility interval provides a range within which we are reasonably confident the true parameter value lies, and the maximum *a posteriori* estimate represents the point in the distribution with the highest posterior probability, serving as a plausible point estimate for the slope parameter. This comprehensive approach allows us to draw informed conclusions regarding the relationship between the age of ancestors and their associated latitudes.

Non-parametric bootstrap Null Hypothesis Significance Test (NHST). As an alternative approach to test our hypothesis under a linear regression framework, we also used the glm function from the R package *stats* v. 3.6.2 (R Core Team 2023) to model node age as a function of reconstructed ancestral latitude, following the formula:

$$Y_{n\,=} = \alpha_{int} + \beta * X_n + \varepsilon_n \qquad (4)$$

where Y_n is the age for each observation at each node n, α_{int} is the intercept, X_n is the estimated ancestral latitude of node n, β is the estimated slope coefficient representing the change in the expected value of Y for a one-unit change in X and ε_n is the error or variation unexplained by other covariates. To find the model with the highest adequacy and fit, we tested combinations of two probability distributions (Gaussian and Gamma) and three link functions (identity, log and inverse) and selected the model with the highest fit (lowest AIC value), highest linearity of predicted *vs* observed values (using qqplots) and better homoscedasticity. When fitting data leveraged from the ML tree, we selected gamma-distributed error and the identity

function (Supplementary Materials 4), whereas for data leveraged from the SVDQ tree, we selected a gaussian distribution with an identity link function (Supplementary Materials 5).

We performed a bootstrap analysis within the NHST framework by conducting 10,000 iterations. For each iteration, we randomized the reconstructed latitude values at the nodes, then performed regression analysis to obtain the slope parameter (β) for each bootstrapped sample. This process generated a null distribution for the slope parameter (β). Given that the observed slope was negative, we calculated the statistical significance (p-value) by finding the proportion of the null distribution that is less than or equal to the observed slope, indicating the probability of getting such a result under the null hypothesis. Following standard statistical procedures, a *p*-value smaller than 0.05 indicates significant evidence against the null hypothesis (no relationship between node age and ancestral latitude).

Results

Specimen-level phylogeny. Following the identification and removal of putative hybrids, we obtained a dataset of 234 accessions for the specimen-level phylogeny (Fig. 1A, Supplementary Fig. 1, Supplementary Table 1). The concatenated alignment was 27,072 bp in length (752 loci) and contained 31.91% missing data. In the ML phylogeny resulting from this dataset, all accessions of a given species formed monophyletic groups except for *Weinmannia reticulata* Ruiz & Pav. ex López. Two different subclades, named *W. reticulata1* and *W. reticulata2,* were treated as separate species for the purpose of the present analysis (Supplementary Fig. 1). Our analysis also included accessions of undetermined species (sp1 to sp6) that showed morphological and phylogenetic cohesion. Further taxonomic treatment will be required to elucidate these species delimitations, which is beyond the scope of the present study but will be the focus of future work. Overall, the

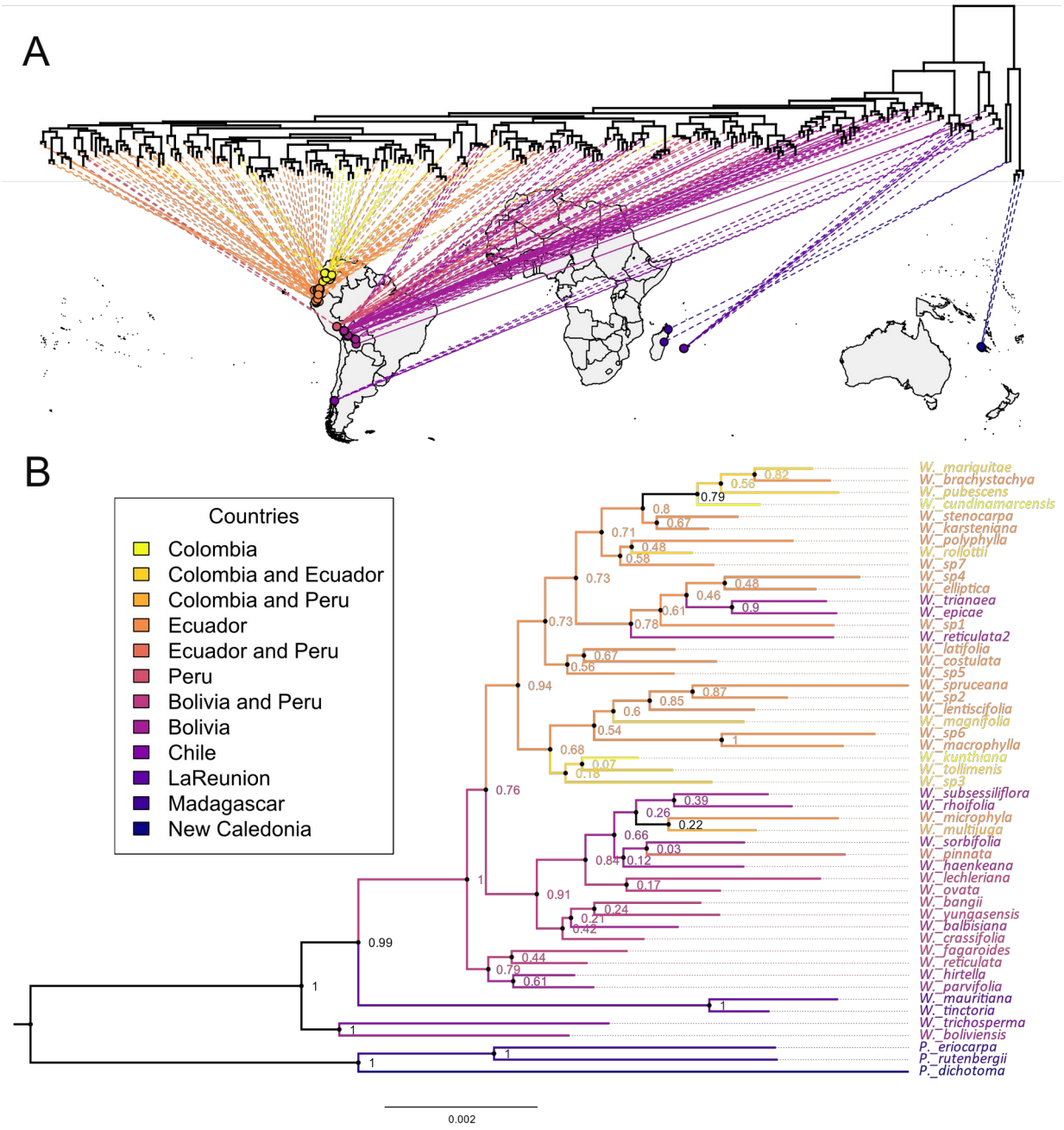

Figure 1. Geographic structure of phylogenetic relationships in *Weinmannia*. A. Specimen-level phylogeny with tips projected onto geographic locations. Maximum Likelihood tree inferred from concatenated 2bRAD-seq data from 234 individuals of *Weinmannia* plus outgroups. Tips labels and, bootstrap support values can be seen in Supplementary Figure 1. **B. Species-level Phylogeny for *Weinmannia*.** Maximum Likelihood tree inferred from concatenated 2bRAD-seq data from 48 individuals of *Weinmannia* plus 3 individuals in the outgroup. Bootstrap support values are shown as node labels, tip labels and branches are colored by country where species were collected.

specimen-level phylogeny showed a strong geographic structure within South American *Weinmannia*, forming clades containing specimens collected in the same region. Species from the Northern Andes (Ecuador and Colombia) formed a clade nested within the *Weinmannia* crown group that included the species sampled from the Central Andes (Bolivia and Peru), Southern Andes (Chile) and Reunion Island (Fig. 1A, Supplementary Fig. 1).

Species-level phylogeny. The final concatenated character matrix for the species-tree (51 tips) reconstruction contained 103,676 bp (2,879 loci) and a 48.63% of missing data. The concatenated ML species tree (ML; Fig. 1B;) and the multi-species coalescent model-based species tree (hereafter SVDQ tree; Supplementary Fig. 2) both showed strong bootstrap support [Bootstrap Support (BS) = 1 in both cases] for genus *Weinmannia*, confirming its monophyly. The time-calibrated phylogeny based on the ML topology showed that the MRCA of the genus *Weinmannia* diverged from the outgroup in the late Eocene around 34.4 Ma and started to diversify ~20.7 Ma (Fig. 2), with similar results observed in the SVDQ tree analysis (~21.38 Ma; Supplementary Fig. 4). Congruent with our specimen-level phylogeny, the species-level phylogenies also showed a general trend where geographically proximal taxa were found in the same clade (Fig. 2; Supplementary Fig. 4).

In the ML species tree, *Weinmannia trichosperma*, the southernmost species located in the temperate, extratropical forests of southern South America, was placed in a clade that was strongly supported as the sister group to the remaining species of *Weinmannia* (BS = 1; Fig. 1B), along with *Weinmannia boliviensis* R. E. Fr. the southernmost species in the central Andes inhabiting the subtropical Tucuman-Bolivian forests. In contrast, our SVDQ tree shows a topology with *W. boliviensis* as a basal branch, followed by a clade consisting of the two Mascarene species, and then *W. trichosperma*, all as successive sister groups to the remaining *Weinmannia* species (supplementary Figs. 2 and 3). Despite the topological differences

between these two trees, both strongly support the placement of the southernmost lineages *W. trichosperma* and *W. boliviensis*, alongside *W. mauritiana* and *W. tinctoria*, as the most basally branching lineages in the phylogeny.

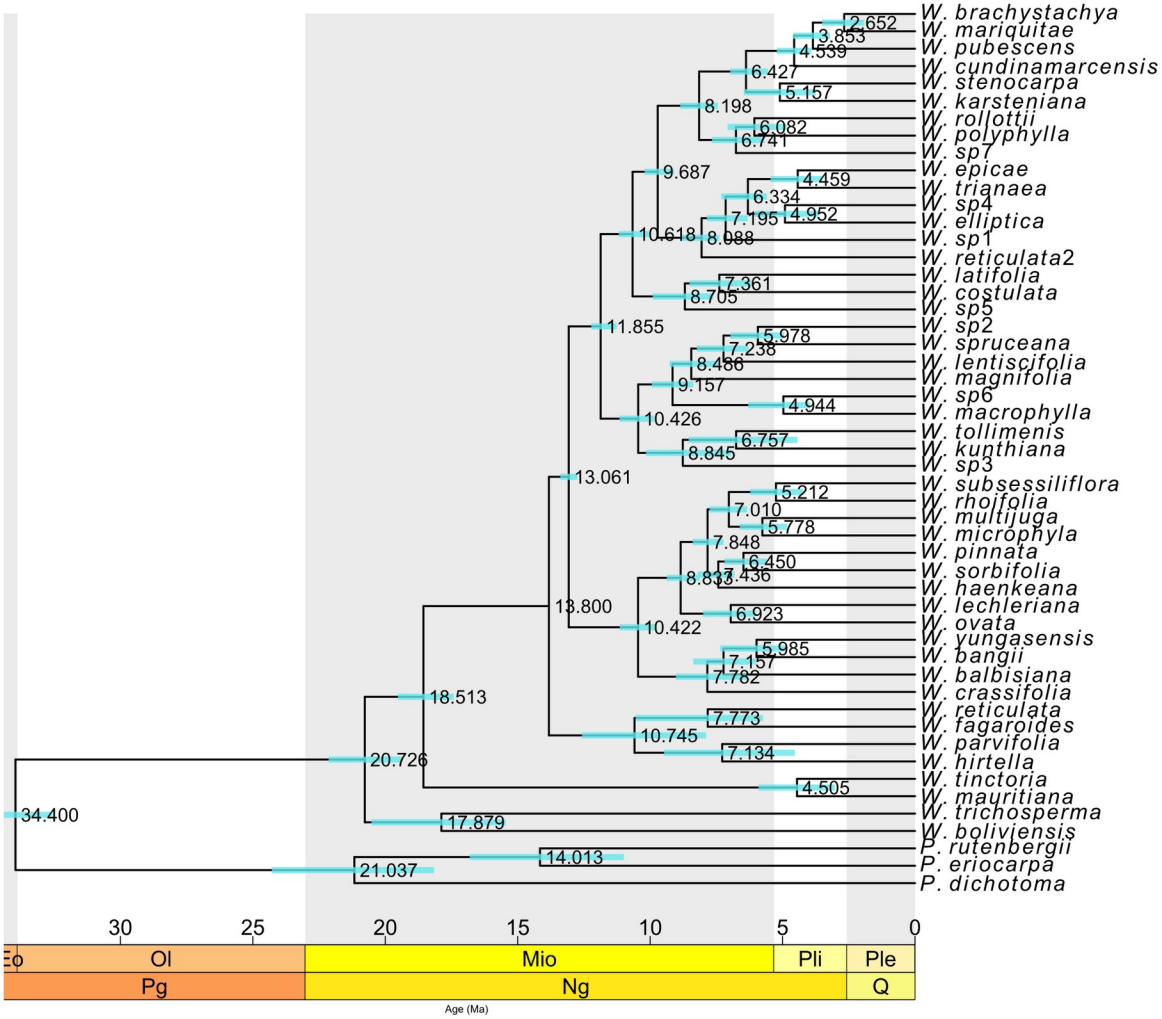

Figure 2. Maximum likelihood phylogeny with estimated divergence times of *Weinmannia* species. Median divergence age estimates across bootstrap trees with 95% confidence intervals in blue bars.

Tropical Andean clade shows geographic structure along the Central and Northern Andes. After the divergence of *Weinmannia* in southern south America and the Mascarenes, the remaining 44 species, which are found exclusively in the tropical Andes, formed a large, strongly supported

clade (BS=1 in Fig. 1B for ML; and BS= 0.98 in Supplementary Fig. 3 for SVDQ), which started to diversify ~13.8 Mya (Fig. 2 and Supplementary Fig. 4). Even accounting for the topological differences among SVDQ and ML, the Tropical Andean clade exhibited clear geographic structure. The ML reconstruction shows two clades at its base, the first containing four species from Bolivia and Peru (BS= 0.79; Fig. 1B), and its sister clade (BS=0.76; Fig. 1B), which bifurcated into two major clades. The first of these clades was strongly supported (BS=0.91; Fig. 1B) and included 13 species from the central Andes, with exceptions such as *Weinmannia multijuga* Killip & A. C. Sm. from Peru and Colombia, *Weinmannia pinnata* L. from Peru and Ecuador, and *Weinmannia microphylla* Ruiz & Pav. from Ecuador. The second of these clades was also well supported (BS = 0.84; Fig. 1B) and included most species from the northern Andes (Ecuador and Colombia), with the exception of *Weinmannia trianea* Wedd., *Weinmannia epicae* A. Fuentes, and what we call *Weinmannia reticulata2* from Bolivia (Fig. 1B).

Our SVDQuartets species tree showed a similar pattern for the Tropical Andes clade, in that it was divided into two major clades. The first contained 16 species, all found in the central Andes of Bolivia and Peru, with the exception of *W. multijuga*, which is found from Colombia to Peru (BS= 0.83, Supplementary Fig. 2). The second clade was well supported (BS=0.84) and contained the remaining 28 species, all from the northern Andes except *W. reticulata2* and *W. balbisiana* Kunth from Bolivia (Supplementary Fig. 2).

Younger clades are distributed towards northern latitudes. Ancestral state reconstructions for latitudes in internal nodes show that the more basal branches are more likely to be associated with higher (*i.e*. more southern) reconstructed latitudes (Fig. 3A and Supplementary Fig. 5A). Likewise, more recently derived nodes are more likely to be associated with lower reconstructed latitudes (*i.e*. more northern).

Our Bayesian model predicting node age as a function of reconstructed latitude on the ML phylogeny yielded a maximum *a posteriori* (MAP) slope for latitude (β) of -0.145. The 79% credible interval estimated

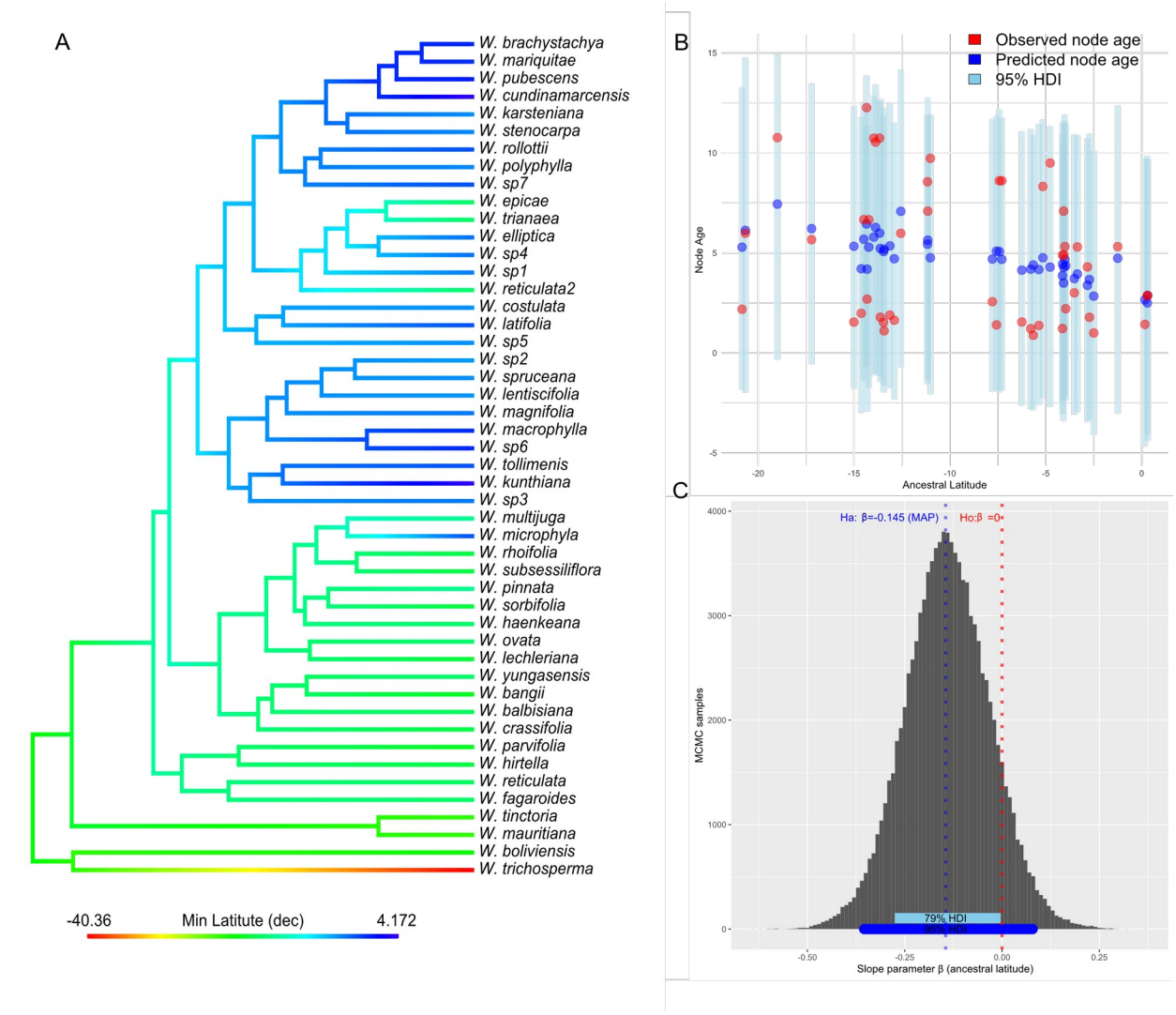

Figure 3. Analysis for testing the dispersal from southern latitudes towards the North Andes though the Andes. A. Ancestral character estimate for latitude of hypothetical ancestors (nodes). Ancestral states were reconstructed on the Maximum likelihood timetree using the minimum latitude of each of the 48 putative *Weinmannia* species considering reviewed accessions. The colors in the figure depict a continuous gradient of latitude, transitioning from southern temperate regions in red to northern tropical regions in blue, with intermediate latitudes in the central Andes represented in green. **B. Bayesian linear regression of node age as a function of predicted ancestral latitude: Posterior predictive check.** Observed values are represented in red dots. The blue dots represent the maximum a posteriori estimates, skyblue bars represent 95% High density intervals (HDI). **C. A posteriori probability distribution for the estimated slope coefficient for latitude as a predictor of node age.** Maximum a posteriori (MAP) is equal to β=-0.145 and the 95%HDI in blue segment goes from to -0.354 to 0.078 which includes cero. However, the 79%HDI goes from -0.276 to -0.003. This result shows the slope is different from zero (β =0) rejecting the null hypothesis with a 79% of credibility.

for this parameter ranged from -0.276 to -0.003, which does not include zero, providing robust evidence to reject the null hypothesis (β=0; Fig. 3C) of no relationship between node age and latitude. Even at a higher 95% credible interval, the value of this parameter ranged from -0.354 to 0.078, showing a strong trend toward negative values (Fig. 3C). Using our SVDQ topology with ML-optimized branch lengths, the more basal nodes tended to be associated with more southern latitudes (MAP for slope = -0.089; Supplementary Fig. 5C), with the null hypothesis rejected with a 60% credible interval ranging from -0.196 to -0.001 (Supplementary Fig. 5C). The results of the null hypothesis significance test using our nonparametric bootstrap on the slope coefficient also showed that node age tended to be negatively related to ancestral latitude when using our ML tree topology (slope = -0.187, p-value = 0.0213). However, when using our SVDQ topology, despite the negative trend of the slope parameter, we did not observe a statistically significant relationship between node age and latitude (slope= -0.107; p-value =0.1466). In summary, both Bayesian and NHST approaches for both the ML and SVDQ inferred topologies, showed a negative slope estimate even though the negative nature of the SVDQ topology was not statistically significant.

Discussion

Our phylogenetic analyses of *Weinmannia* show that extratropical species are preferentially placed at the base of the evolutionary tree. We also find a negative relationship between the age of clades and their latitudinal distribution across the phylogeny. This suggests that *Weinmannia* probably originated from a lineage that was pre-adapted to the climatic conditions of the southern extratropics, and that the diversification of *Weinmannia* in the American tropics occurred concomitantly with south-to-north dispersal when suitable climates were created as a result of the Andean uplift.

An extratropical origin for *Weinmannia*

Our ML phylogeny places *Weinmannia trichosperma* from the temperate forests of southern South America as sister to all the other species of the genus *Weinmannia* (ML, BS = 1, Fig. 1). This is consistent with previous morphological and genetic reconstructions of the phylogenetic relationships of species in the genus (Bradford, 1998, 2002), but is slightly different from results with our SVDQ approach (Supplementary Fig. 2). The paleontological evidence is also consistent with this basal placement of *W. trichosperma* and suggests that the lineage had a widespread distribution in the southern extratropics during the Paleogene. For example, an early Oligocene (~30 Ma) macrofossil record, *Weinmanniaphyllum bernardii* R.J.Carp. & A.M.Buchan from extratropical Tasmania (Carpenter and Buchanan 1993), where the genus is now extinct, is morphologically similar to *W. trichosperma* (Bradford, 1998, but see Bradford et al. 2001). Still, the extinction of the genus outside of its modern range in the Americas and the Mascarenes may be related to a sharp reduction in forest cover due to the formation of the Antarctic Ice Sheet in the early Oligocene, which has been associated with a massive extinction of the Austral paleoflora across the southern hemisphere (Francis, 1996; Truswell and Macphail, 2009). This massive extinction process may also explain why this old, basal clade [stem age 20.7 Ma] is currently relatively poor in species richness (Fig. 1, 2), despite showing evidence of having a wider geographic distribution in the past (Crisp and Cook, 2009; Antonelli and Sanmartín, 2011b).

Also consistently placed among the basally diverging lineages is the subtropical species *Weinmannia boliviensis* (Fig. 1a and S2). *W. boliviensis* is distributed in the Tucuman-Bolivian forests (Harling and Fuentes, 2014), which are subtropical montane forests on the eastern slope of the Andes, extending from 23°S to 29°S (Cabrera, 1976, Olson et al. 2001). Interestingly, even though the forests harboring *W. boliviensis* are disjunct from those harboring *W. trichosperma* in southern South America and

contiguous with those of the Andean lower latitudes, *W. boliviensis* is phylogenetically closer to *W. trichosperma* than to species in the central Andes (Fig. 1). Furthermore, *W. trichosperma* and *W. boliviensis* differ morphologically. For example, *W. boliviensis* has simple leaves whereas *W. trichosperma* has compound leaves (Harling and Fuentes, 2014). According to our ML phylogeny, *W. boliviensis* and *W. trichosperma* diverged during the Miocene, 17.9 Ma (Fig. 2). This date precedes the final uplift of the central and southern Andes to their present elevations (above 3000 m), which began during the late Miocene (~11 Ma) (Gregory-Wodzicki, 2000; Siravo et al. 2018), and the subsequent expansion of arid areas to the west and east of the mountain range (the southern arid diagonal of South America; Rambo, 1952, 1953). Therefore, the evolutionary divergence of the base of *Weinmannia* would have occurred in forests composed of Gondwanan lineages that persisted in South America during the Paleogene and Neogene (Romero, 1986). These extratropical paleoforests were isolated from the tropical lowland flora of South America by environmental rather than geographic factors (Jaramillo and Cárdenas, 2013) and accumulated their own evolutionary uniqueness (Segovia et al. 2020a). Finally, the species of these forests would have been largely extinguished in the lowlands as a result of the intensification of aridity triggered by the Andean orogeny, leaving remnants in specific locations along the Pacific coast of southern South America, on the Brazilian plateau, and on the slopes of the tropical Andean mountain range, where the genus *Weinmannia* is now restricted (Villagran and Hinojosa, 1997, 2005).

Expanded species sampling, combined with improved phylogenetic resolution, has led to an improved understanding of the origin of the *Weinmannia* clade in the tropical Andes. Bradford (2002) used a maximum of six species from the tropical Andes to reconstruct phylogenetic relationships, using chloroplast and nuclear markers. In contrast, we included 45 species from this region (Fig. 1) and a much greater number of variable loci distributed throughout the genome. Moreover, our approach provides

much greater resolution than a previous study that employed similar genomic approaches (Angiosperms353) but sampled only one *Weinmannia* species from tropical America (Pillon et al. 2021). Likewise, formal analyses to test the relationship between node age and latitude help resolve the direction of the dispersal of *Weinmannia.* The Bayesian approach to infer the direction of migration in *Weinmannia* provides robust results because it avoids binary decisions (e.g. using p-values) and provides a continuum of evidence, which reduces the risk of fixed thresholds prone to type I and type II errors.

South-to-North dispersal through the Andean Corridor

The negative relationship between node age and latitude in our phylogeny reveals a late arrival of the lineage in the tropics and a south-to-north dispersal route along the Andes (Fig. 3 and Supplementary Figs. 5 and 6). We propose that as the Andean uplift created an environmental corridor at mid and high elevations throughout of South America, *Weinmannia* gradually expanded its range from south to north. This scenario is consistent with fossil evidence documenting the oldest pollen records of *Weinmannia* in the northern Andes are from the late Pliocene and Pleistocene (1.5–3.2 Ma) (Van der Hammen et al. 1973, Hooghiemstra 1989). The crown age of the Northern Andes clade recovered in the present study is estimated at 11.9 Ma (Fig. 2), predating the earliest fossil evidence for *Weinmannia* in the region by several million years. This inconsistency may be due to the low preservation potential of the pollen or sampling intensity in the fossil record, which can cause the date of first fossil appearance to be significantly younger than the true arrival date of a taxon in a region (Smith and Peterson, 2002).

The dispersal route of *Weinmannia* suggests that the lineage evolved first under the environmental conditions of the southern extratropics and maintained the acquired adaptations during south-to-north dispersal. Plant lineages often exhibit a high degree of phylogenetic niche conservatism (Crisp et al. 2009), and this tendency likely allowed *Weinmannia* and other

extratropical lineages to rapidly colonize the similar environments created at mid- and high-elevations following the uplift of the Andes at tropical latitudes (Donoghue, 2008; Segovia and Armesto, 2015). Moreover, modern patterns of phylogenetic turnover across elevational gradients along the tropical Andes reveal a significant influence of ecological sorting of pre-adapted clades in shaping tree communities (Ramírez et al. 2019; Griffiths et al. 2020; Linan et al. 2021a). This suggests that the route taken by *Weinmannia* would have been a general corridor of environmentally driven immigration of plant lineages into the tropical Andes. Although the environmental factors currently driving phylogenetic turnover and shaping the biogeographic corridor in the past have not been directly tested, the presence of freezing temperatures in a regular year may have some influence. On the one hand, freezing temperatures drive taxonomic turnover and differentiate lower and higher elevation montane forests in the northern Andes (Pérez-Escobar et al. 2022). On the other hand, phylogenetic similarities of tree assemblages along the Americas unveil a biological corridor that is differentiated by whether freezing temperatures occur regularly (Segovia et al. 2020a). Therefore, the current taxonomic and phylogenetic turnover, and thus the historical corridor shaped by freezing temperatures in the tropical Andes, may exemplify the global pattern of conservative evolution (Zanne et al. 2014) and distribution of frost tolerance in plants (Wiens and Donoghue, 2004).

The tree topologies differed somewhat between RAxML and SVDQ. These differences in phylogenetic tree topologies when using SVDquartet and RAxML (Supplementary Fig. 3) may be due to their different underlying principles and methodologies. SVDquartets uses a quartet-based approach that relies on gene coalescence patterns without imposing specific evolutionary models, allowing it to account for complex evolutionary signals such as incomplete lineage sorting or hybridization. In contrast, RAxML is a maximum likelihood-based method that operates under defined evolutionary models to estimate relationships and branch lengths, potentially yielding a

simpler tree structure. Despite the differences in methods, the overarching patterns remain robust across phylogenetic reconstruction approaches, with both SVDquartets and RAxML revealing similar geographic structures. Both methods consistently identified a clade containing nearly all species from the northern Andes nested within a broader clade containing all species from the tropical Andes (Fig. 1 and Supplementary Fig. 2). Although the trees show slight differences in statistical support, the observed trend of northern lineages appearing more recently suggests that lineage dispersal likely followed a northward progression through the Andes (Fig. 3 and Supplementary Figs. 5 and 6).

The intriguing history of the Mascarenes' *Weinmannia*

Our ML phylogeny shows that a small clade containing two species from the western Indian Ocean, *Weinmannia tinctoria* Sm. and *Weinmannia mauritania* D.Don, is nested within South American *Weinmannia* (Fig. 1 and Supplementary Fig. 2). This result confirms previous phylogenetic reconstructions (Bradford, 2002), but differs from results obtained with our SVDQ approach (Supplementary Fig. 2). This result is surprising because it implies a long-distance dispersal event that occurred after the last tropical-extratropical dispersal event for the lineage within South America, according to our time-calibrated ML phylogeny (Fig. 2). Although cumulative evidence shows high levels of intercontinental dispersal in tropical biomes (Givnish and Renner, 2004, Gagnon et al. 2019), this result is still surprising because the stem age (~18.513 Ma, Fig. 2 and ~ 19.749 Ma, Supplementary Fig. 4) of the Mascarene clade is older than the volcanic origin of the archipelago (less than 8 Ma, McDougall and Chamalaun, 1969; McDougall, 1971). Furthermore, this result is unusual because botanical affinities and phylogenetic evidence suggest that Madagascar may have acted as a source of diversity for the Mascarenes (Cadet, 1977; Linan et al. 2019), but no species of *Weinmannia* are currently found in Madagascar or Africa (Pillon

et al. 2021). Thus, any model for the dispersal of *Weinmannia* from South America can only be proposed if Madagascar or Africa are involved as a cryptic stepping-stone to reach the Mascarenes. In any case, further studies are needed to properly address this intriguing disjunction and to clarify possible vicariant or long-distance dispersal events in the origin of the genus *Weinmannia*.

Conclusion

Weinmannia reflects a pattern in which the area of lineage origin is poorer in species richness than the recently colonized area (e.g., 1 species in the extratropics, 2 species in the subtropics, and more than 70 species in the tropical Andes). This pattern, likely due to massive extratropical extinctions and recent diversification in the tropics, has also been proposed for the entire family Cunoniaceae (Segovia et al. 2020b, Pillon et al. 2021), which has traditionally been considered a lineage derived from the "Gondwanan" center of plant diversification (Raven and Axelrod, 1974; Mildenhall, 1980; Hill, 1994). Furthermore, the fossil record indicates that the Cunoniaceae family was present in Antarctica (i.e., western Gondwana) during the Late Cretaceous (~70 Ma) (Poole et al. 2000), along with a highly diverse vegetation similar in taxonomic composition to the temperate forests of southern South America today (Poole et al. 2003). This suggests that the biogeographic history of *Weinmannia* and Cunoniaceae may have been shared with other lineages from the so-called Austral Floristic Realm (Morrone, 2002; Moreira-Muñoz, 2007). Thus, our results provide insight into an overlooked and seemingly counterintuitive phenomenon: the taxonomic and phylogenetic enrichment of the hyperdiverse tropical Andean floras by the immigration of remnant lineages from the ancient southern extratropical floras of the Southern Hemisphere.

Acknowledgements

The study was supported by FONDECYT 11200967 and the National Science Foundation (DEB 1836353). R.A.S is supported by Institute of Ecology and Biodiversity (IEB) ANID grant FB210006, F.F.G. was supported by the Shirley A. Graham Fellowships in Systematic Botany and Biogeography of the Missouri Botanical Garden. C.E.E. and the Conservation Genetics Program at the Missouri Botanical Garden is supported by donations from Stephen and Camilla Brauer, Philip and Sima Needleman, and the Bellwether Foundation. Collections in Ecuador were partially funded by Universidad Tecnológica Indoamérica, NHO. We thank the Ministerio del Ambiente, Agua y Transición Ecológica in Ecuador for collecting permits (contrato marco MAE-DNB-CM-2019-011).

References

Acha S., Linan A., MacDougal J., Edwards C. 2021. The evolutionary history of vines in a neotropical biodiversity hotspot: Phylogenomics and biogeography of a large passion flower clade (Passiflora section Decaloba). *Mol. Phylogenetics Evol*. 164:107260.

Andrews S. 2010. FastQC: a quality control tool for high throughput sequence data. Available from http://www.bioinformatics.babraham.ac.uk/projects/fastqc.

Antonelli A., Sanmartín I. 2011a. Why are there so many plant species in the Neotropics? *Taxon* 60:403–414.

Antonelli A,, Sanmartín I. 2011b. Mass extinction, gradual cooling, or rapid radiation Reconstructing the spatiotemporal evolution of the ancient angiosperm genus *Hedyosmum* (Chloranthaceae) using empirical and simulated approaches. *Syst. Biol.* 60:596–615.

Antonelli A., Zizka A., Silvestro D., Scharn R., Cascales-Miñana B., Bacon C. D. 2015. An engine for global plant diversity: highest evolutionary turnover and emigration in the American tropics. *Frontiers in Genetics* 6:130.

Bacon C.D., Velásquez-Puentes F.J., Hinojosa L.F., Schwartz T., Oxelman B., Pfeil B., Arroyo M.T.K., Wanntorp L., Antonelli A. 2018. Evolutionary persistence in *Gunnera* and the contribution of southern plant groups to the tropical Andes biodiversity hotspot. *PeerJ* 6: e4388.

Balslev H. 1993. Introduction. In: Balslev H., editor, *Neotropical Montane Forests – Biodiversity and Conservation*. Aarhus, Denmark: AUU Reports 31, Aarhus University Press.

Barnes R.W. 1999. Palaeobiogeography, extinctions and evolutionary trends in the Cunoniaceae: a synthesis of the fossil record (thesis). University of Tasmania. https://doi.org/10.25959/23246864.v1.

Bell C. D., Donoghue M. J. 2005. Phylogeny and biogeography of Valerianaceae (Dipsacales) with special reference to the South American valerians. *Org. Divers. Evol.* 5: 147-159.

Berry E.W. 1917. The Age of the Bolivian Andes. *Proc. Natl. Acad. Sci. U.S.A.* 3:283–285.

Bradford J.C. 1998. A cladistic analysis of species groups in *Weinmannia* (Cunoniaceae) based on morphology and inflorescence architecture. *Ann. Missouri Bot. Gard.* 85:565-593.

Barnes R. W., Hill R. S., & Bradford, J. C. 2001. The history of Cunoniaceae in Australia from macrofossil evidence. *Australian Journal of Botany* 49:301-320.

Bradford J.C. 2002. Molecular phylogenetics and morphological evolution in Cunonieae (Cunoniaceae). *Ann. Missouri Bot. Gard.* 89:491-503.

Bradford J. C., Fortune-Hopkins H. C. Barnes R. W. 2004 *Cunoniaceae*. In The families and genera of vascular plants (ed. K. Kubitzki), pp. 91–111. Heidelberg, Germany: Springer.

Cabrera A.L. 1976. Regiones fitogeográficas argentinas. *Enciclopedia Argentina de Agricultura y Jardinería* 2:1-85.

Cadet L.J.T. 1980. *La végétation de l'île de la Réunion: étude phytoécologique et phytosociologique* (Doctoral dissertation, Impr. Cazal).

Carpenter R.J., Buchanan A.M. 1993. Oligocene leaves, fruit and flowers of the Cunoniaceae from Cethana, Tasmania. *Aust. Syst. Bot.* 6:91-109.

Carpenter B., Gelman A., Hoffman M.D., Lee D., Goodrich B., Betancourt M., Brubaker M., Guo J., Li P., Riddell A. 2017. Stan: A Probabilistic Programming Language. *J. Stat. Soft*. 76:1–32.

Castiglione S., Tesone G., Piccolo M., Melchionna M., Mondanaro A., Serio C., Di Febbraro M., Raia P. 2018. A new method for testing evolutionary rate variation and shifts in phenotypic evolution. *Methods in Ecology and Evolution* 9:974–983.

Chifman J., Kubatko L., 2014. Quartet Inference from SNP Data Under the Coalescent Model. *Bioinformatics* 30:3317–3324.

Crisp MD, Cook LG. 2009. Explosive radiation or cryptic mass extinction? Interpreting signatures in molecular phylogenies. *Evolution* 63:2257–2265.

Crisp M. D., Arroyo M. T., Cook L. G., Gandolfo M. A., Jordan G. J., McGlone M. S., Weston P.H., Westoby M., Wilf P., Linder H. P. 2009. Phylogenetic biome conservatism on a global scale. *Nature* 458: 754-756.

Dellinger A. S., Lagomarsino L., Michelangeli, F., Dullinger S., Smith S. D. 2024. The Sequential Direct and Indirect Effects of Mountain Uplift,

Climatic Niche, and Floral Trait Evolution on Diversification Dynamics in an Andean Plant Clade. *Systematic Biology*: syae011.

Donoghue M.J. 2008. A phylogenetic perspective on the distribution of plant diversity. *Proc. Natl. Acad. Sci.* 105:11549-11555.

Donoghue M.J., Eaton D.A.R., Maya-Lastra C.A., Landis M.J., Sweeney P.W., Olson M.E., Cacho N.I., Moeglein M.K., Gardner J.R., Heaphy N.M., Castorena M., Rivas A.S., Clement W.L. Edwards E.J. 2022. Replicated radiation of a plant clade along a cloud forest archipelago. *Nat Ecol Evol* 6: 1318–1329.

Doyle J.J., Doyle J.L. 1987. A rapid DNA isolation procedure for small quantities of fresh leaf tissue. *Phytochem. Bull*. 19:11–15.

Drummond A. J. Rambaut A.2007. BEAST: Bayesian evolutionary analysis by sampling trees. *BMC Evol. Biol.* 7:214.

Earl D.A., von Holdt B.M. 2012. STRUCTURE HARVESTER: a website and program for visualizing STRUCTURE output and implementing the Evanno method. *Conserv. Genet. Resour*. 4: 359-361.

Eaton D.A.R., Overcast I. 2020. ipyrad: interactive assembly and analysis of RADseq datasets. *Bioinformatics.* 36:2592–2594.

Francis J.E. 1996. Antarctic palaeobotany: clues to climate change. *Terra Antarctica* 3:135–140.

Gagnon E., Ringelberg J.J., Bruneau A., Lewis G P., Hughes C.E. 2019. Global succulent biome phylogenetic conservatism across the pantropical Caesalpinia group (Leguminosae). *New Phytol*. 222:1994-2008.

Gentry A.H. 1982. Neotropical floristic diversity: phytogeographical connections between Central and South America, Pleistocene climatic fluctuations, or an accident of the Andean orogeny? *Ann. Missouri Bot. Gard*. 69:557–593.

Gentry A.H. 1995. Patterns of diversity and floristic composition in Neotropical montane forests. In: S.P. Churchill, H. Balslev, E. Forero, J. Lutein, editors. *Biodiversity and Conservation of Neotropical Montane Forests.* Nueva York, USA: New York Botanical Garden. p. 103-126.

Givnish T.J., Renner S.S. 2004. Tropical Intercontinental Disjunctions: Gondwana Breakup, Immigration from the Boreotropics, and Transoceanic Dispersal. *Int. J. Plant Sci.* 165:S1-S6.

Givnish T.J., Barfuss M.H.J., Van Ee B., Riina R., Schulte K., Horres R., Gonsiska P.A., Jabaily R.S., Crayn D.M., Smith J.A.C., Winter K., Brown G.K., Evans T.M., Holst B.K., Luther H., Till W., Zizka G., Berry P.E., Systma K.J.. 2014. Adaptive radiation, correlated and contingent evolution, and net species diversification in Bromeliaceae. *Mol. Phylogenet. Evol.* 71:55–78

González-Caro S., Duque Á., Feeley K.J., Cabrera E., Phillips J., Ramirez, S., Yepes A. 2020. The legacy of biogeographic history on the composition and structure of Andean forests. *Ecology* 101:e03131.

González-Caro S., Tello J.S., Myers J.A., Feeley K., Blundo C., Calderón-Loor M., Carilla J., Cayola L., Cuesta F., Farfán W., Fuentes A.F., García-Cabrera K., Grau R., Idarraga Á., Loza M.I., Malhi Y., Malizia A., Malizia L., Osinaga-Acosta O., Pinto E., Salinas N., Silman M., Terán-Valdéz A., Duque Á. 2023. Historical Assembly of Andean Tree Communities. *Plants* 12:3546.

Graham, A. 1973. History of the arborescent temperate element in the northern Latin American biota. Vegetation and vegetational history of northern Latin America, 301-314.

Graham, A. 1995. Development of affinities between Mexican/Central American and northern South American lowland and lower montane vegetation during the Tertiary. Pp. 11-22 in S. P. Churchill, H.

Balslev, E. Forero & J. L. Luteyn (editors), Biodiversity and Conservation of Neotropical Montane Forests. New York Botanical Garden, Bronx.

Graham A., Gregory-Wodzicki K.M., Wright K.L. 2001. Studies in Neotropical Paleobotany. XV. A Mio-Pliocene palynoflora from the Eastern Cordillera, Bolivia: implications for the uplift history of the Central Andes. *American Journal of Botany* 88, 1545–1557.

Gregory-Wodzicki K.M. 2000. Uplift history of the Central and Northern Andes: a review. *Geol. Soc. Am. Bull.* 112:1091-1105.

Griffiths A.R., Silman M.R., Farfán Rios W., Feeley K.J., García Cabrera K., Meir P., Salinas N., Dexter K.G. 2020. Evolutionary heritage shapes tree distributions along an Amazon-to-Andes elevation gradient. *Biotropica* 53:38–50.

Harling G.W. Fuentes A.F. 2014. Cunoniaceae. In: P.M. Jørgensen, M.H. Nee, S.G. Beck, editors. *Cat. Pl. Vasc. Bolivia, Monogr. Syst. Bot. Missouri Bot. Gard. 127*. St. Louis.USA. Missouri Botanical Garden Press:540–542.

Hazzi N. A., Moreno J. S., Ortiz-Movliav C., Palacio R. D. 2018. Biogeographic regions and events of isolation and diversification of the endemic biota of the tropical Andes. *Proceedings of the National Academy of Sciences* 115: 7985-7990.

Hill A.W. 1929. Antarctica and problems in geographical distribution. *International Congress of Plant Sciences* 2:1477–1486.

Hill R.S. 1994. *History of the Australian vegetation: Cretaceous to Recent*. Cambridge University Press, Cambridge, UK.

Hooghiemstra H. 1984. Vegetational and climatic history of the high plain of Bogotá, Colombia: A continuous record of the last 3.5 million years. *Diss. Bot.* 79:368.

Hooghiemstra H. 1989. Quaternary and upper-pliocene glaciations and forest development in the tropical Andes: Evidence from a long high-resolution pollen record from the sedimentary basin of Bogotá, Colombia. *Palaeogeogr. Palaeoclimatol. Palaeoecol.* 72:11–26.

Inglis P.W., Pappas M., Resende L.V., Grattapaglia D. 2018. Fast and inexpensive protocols for consistent extraction of high quality DNA and RNA from challenging plant and fungal samples for high-throughput SNP genotyping and sequencing applications. *PLoS ONE* 13: e0206085.

Jaramillo C., Cardenas A. 2013. Global warming and neotropical rainforests: a historical perspective. *Annu. Rev. Earth Pl. Sc.* 41:741–766.

Lagomarsino L.P., Condamine F.L., Antonelli A., Mulch A., Davis C.C. 2016. The abiotic and biotic drivers of rapid diversification in Andean bellflowers (Campanulaceae). *New Phytol*. 210: 1430–1442.

Lemoine F., Domelevo Entfellner J.-B., Wilkinson E., Correia D., Dávila Felipe M., De Oliveira T., Gascuel O. 2018. Renewing Felsenstein's phylogenetic bootstrap in the era of big data. *Nature* 556:452–456.

Linan A.G., Schatz G.E., Lowry P.P., Miller A., Edwards C. E. 2019. Ebony and the Mascarenes: the evolutionary relationships and biogeography of *Diospyros* (Ebenaceae) in the western Indian Ocean. *Bot. J. Linn. Soc*. 190: 359-373.

Linan A.G., Myers J.A., Edwards C.E., Zanne A.E., Smith S.A., Arellano G., ... Tello J. S. 2021a. The evolutionary assembly of forest communities along environmental gradients: recent diversification or sorting of pre-adapted clades?. *New Phytol.* 232(6): 2506-2519.

Linan A.G., Lowry II P.P., Miller A.J., Schatz G.E., Sevathian J.-C., Edwards C.E. 2021b. RAD-sequencing reveals patterns of diversification and hybridization, and the accumulation of reproductive isolation in a

clade of partially sympatric, tropical island trees. *Molecular Ecology* 30: 4520–4537.

Lindtke, D., Gompert, Z., Lexer, C., & Buerkle, C. A. 2014. Unexpected ancestry of Populus seedlings from a hybrid zone implies a large role for post zygotic selection in the maintenance of species. *Molecular Ecology*, 23, 4316–4330.

Luebert F., Weigend M. 2014. Phylogenetic insights into Andean plant diversification. *Front. Ecol. Evol. 2*:27.

Mashburn B., Jhangeer-Khan R., Bégué A., Tatayah V., Olsen K.M., Edwards C.E. 2023. Genetic assessment improves conservation efforts for the critically endangered oceanic island endemic *Hibiscus liliiflorus*. *J. Hered.* 114:259–270.

Maurin K.J.L. 2008. An empirical guide for producing a dated phylogeny with treePL in a maximum likelihood framework.

McDougall I.A.N., Chamalaun F.H. 1969. Isotopic dating and geomagnetic polarity studies on volcanic rocks from Mauritius, Indian Ocean. *Geol. Soc. Am. Bull.* 80:1419-1442.

McDougall I. 1971. The geochronology and evolution of the young volcanic island of Réunion, Indian Ocean. *Geochim. Cosmochim. Acta* 35:261-288.

Mildenhall D.C. 1980. New Zealand Late Cretaceous and Cenozoic plant biogeography: a contribution. *Palaeogeogr. Palaeoclimatol. Palaeoecol.* 31:197-233.

Moreira-Muñoz A. 2007. The Austral floristic realm revisited. *Journal of Biogeography* 34:1649–1660.

Morrone J.J. 2002. Biogeographical regions under track and cladistic scrutiny. Journal of Biogeography 29: 149–152.

Myers N., Mittermeier R., Mittermeier C., da Fonseca G.A.B., Kent J. 2000. Biodiversity hotspots for conservation priorities. *Nature* 403:853–858.

Neves D.M., Dexter K.G., Baker T.R., Coelho de Souza F., Oliveira-Filho A.T., Queiroz, L.P., Lima H.C., Simon M.F., Lewis G.P., Segovia R.A., Arroyo L., Reynel C., Marcelo-Peña J.L., Huamantupa-Chuquimaco I., Villaroel D., Parada G.A., Daza A., Linares-Palomino R., Ferreira L.V., Salomão R.P., Siqueira G.S., Nascimento M.T., Fraga C.N., Pennington R.T. 2020. Evolutionary diversity in tropical tree communities peaks at intermediate precipitation. *Sci. Rep.* 10:1188.

Olson D.M., Dinerstein E., Wikramanayake E.D., Burgess N.D., Powell G.V., Underwood E.C., D'amico J.A., Itoua I., Strand H.E., Morrison J.C., Loucks C.J., Allnutt T.F., Ricketts T.H., Kura Y., Lamoreux J.F., Wettengel W.W., Hedao P., Kassem K.R. 2001. Terrestrial Ecoregions of the World: A New Map of Life on Earth: A new global map of terrestrial ecoregions provides an innovative tool for conserving biodiversity. *BioSci*. 51:933-938.

Owusu, S. A., Sullivan, A. R., Weber, J. R., Hipp, A. L., & Gailing, O. 2015. Taxonomic relationships and gene flow in four NorthAmerican Quercus Species (Quercus section Lobatae). *Systematic Botany*, 40(2), 510–521.

Paris J.R., Stevens J.R., Catchen J.M. 2017. Lost in parameter space: a road map for stacks. *Methods Ecol. Evol.* 8:1360–1373.

Pennington R.T., Dick C.W. 2004. The role of immigrants in the assembly of the South American rainforest tree flora. *Philosophical Transactions of the Royal Society of London. Series B: Biological Sciences* 359:1611-1622.

Pérez-Escobar O.A., Chomicki G., Condamine F.L., Karremans A.P., Bogarín D., Matzke N.J., Silvestro D., Antonelli A. 2017. Recent origin and

rapid speciation of Neotropical orchids in the world's richest plant biodiversity hotspot. *New Phytol.* 215:891–905.

Pérez-Escobar O.A., Zizka A., Bermúdez M.A., Meseguer A.S., Condamine F.L., Hoorn C., Hooghiemstra H., Pu Y., Bogarín D., Boschman L.M., Pennington R.T., Antonelli A., Chomicki G. 2022. The Andes through time: evolution and distribution of Andean floras. *Trends Plant Sci.* 27:364-378.

Pillon Y., Hopkins H.C., Maurin O., Epitawalage, N., Bradford, J., Rogers, Z.S., Baker W.J., Forest, F. 2021. Phylogenomics and biogeography of Cunoniaceae (Oxalidales) with complete generic sampling and taxonomic realignments. *Am. J. Bot.* 108:1181-1200.

Poole I., Cantrill D.J., Hayes P., Francis J. 2000. The fossil record of Cunoniaceae: new evidence from Late Cretaceous wood of Antarctica?. *Rev. Palaeobot. Palynol.* 111:127-144.

Poole I., Mennega A.M., Cantrill D.J. 2003. Valdivian ecosystems in the Late Cretaceous and Early Tertiary of Antarctica: further evidence from myrtaceous and eucryphiaceous fossil wood. *Rev. Palaeobot. Palynol.* 124:9-27.

Pritchard J.K., Stephens M., Donnelly P. 2000. Inference of Population Structure Using Multilocus Genotype Data. *Genetics* 155:945–959.

Quiroga M.P., Mathiasen P., Iglesias A., Mill R.R., Premoli A.C. 2016. Molecular and fossil evidence disentangle the biogeographical history of Podocarpus, a key genus in plant geography. *J. Biogeogr.* 43:372-383.

R Core Team. 2023. R: A Language and Environment for Statistical Computing. R Foundation for Statistical Computing, Vienna, Austria. https://www.R-project.org/.

Rahbek C., Borregaard M., Antonelli A., Colwell R., Holt B., Nogués-Bravo D., Rasmussen C., Richardson K., Rosing M., Whittaker R., Fjeldså J. (2019). Building mountain biodiversity: Geological and evolutionary processes. *Science* 365:1114-1119.

Rambo B. 1952. Analise geografica das compostas sul-brasileras. *Sellowia* 5:87–159.

Rambo B. 1953. Historia da flora do Planalto Riograndense. *Sellowia* 5:185–232.

Ramírez S., González-Caro S., Phillips J., Cabrera E., Feeley K.J., Duque Á. 2019. The influence of historical dispersal on the phylogenetic structure of tree communities in the tropical Andes. *Biotropica* 51:500-508.

Raven P.H., Axelrod D.I. 1974. Angiosperm biogeography and past continental movements. *Ann. Missouri Bot. Gard*. 61:539-673.

Revell L.J. 2012. phytools: an R package for phylogenetic comparative biology (and other things). *Methods Ecol. Evol.* 3:217–223.

Romero E.J. 1986. Paleogene phytogeography and climatology of South America. *Ann. Missouri Bot. Gard*. 73:449–461.

Schwery O., Onstein R.E., Bouchenak-Khelladi Y., Xing Y., Carter R.J., Linder H.P. 2015. As old as the mountains: the radiations of the Ericaceae. *New Phytol.* 207:355–367.

Segovia R.A., Armesto J.J. 2015. The Gondwanan legacy in South American biogeography. *J. Biogeogr.* 42:209-217.

Segovia R.A., Pennington R.T., Baker T.R., Coelho de Souza F., Neves D.M., Davis C.C., Armesto J.J., Olivera-Filho A.T., Dexter, K. G. 2020a. Freezing and water availability structure the evolutionary diversity of trees across the Americas. *Sc. Adv.* 6:eaaz5373.

Segovia R.A., Griffiths A.R., Arenas D., Dias A.P., Dexter K.G. 2020b. Signals of recent tropical radiations in Cunoniaceae, an iconic family for understanding Southern Hemisphere biogeography. *bioRxiv* 2020-01.

Siravo G., Fellin M.G., Faccenna C., Bayona G., Lucci F., Molin P., Maden C. 2018. Constraints on the Cenozoic deformation of the northern Eastern Cordillera, Colombia. *Tectonics* 37:4311-4337.

Smith A.B., Peterson K.J. 2002. Dating the time of origin of major clades: molecular clocks and the fossil record. *Annu. Rev. Earth Planet. Sci.* 30: 65-88.

Smith S.A., O'Meara B.C. 2012. treePL: divergence time estimation using penalized likelihood for large phylogenies. *Bioinformatics* 28:2689–2690.

Spriggs E.L., Clement W.L., Sweeney P.W., Madriñán S., Edwards E.J, Donoghue M.J. 2015. Temperate radiations and dying members of a tropical past: the diversification of *Viburnum*. *New Phytol.* 207: 340–354.

Stamatakis A., 2014. RAxML version 8: a tool for phylogenetic analysis and post-analysis of large phylogenies. *Bioinformatics* 30:1312–1313.

Stan Development Team. 2023. RStan: the R interface to Stan. R package version 2.26.23. https://mc-stan.org/.

Tietje M., Antonelli A., Forest F., Govaerts R., Smith S.A., Sun, M., Baker W.J. Eiserhardt W.L. 2023. Global hotspots of plant phylogenetic diversity. *New Phytol*. 240: 1636-1646.

Truswell E.M., Macphail M.K. 2009. Polar forests on the edge of extinction: what does the fossil spore and pollen evidence from East Antarctica say? *Aust. Syst. Bot.* 22:57–106.

Ulloa-Ulloa C., Acevedo-Rodríguez P., Beck S., Belgrano M.J., Bernal R., Berry P.E., Brako L., Celis M., Davidse G., Forzza R.C., Gradstein S.R., Hokche O., León B., León-Yánez S., Magill R.E., Neill D.A., Nee M., Raven P.H., Stimmel H., Strong M.T., Villaseñor J.L., Zarucchi J.L., Zuloaga F.O., Jørgensen P.M. 2017. An integrated assessment of the vascular plant species of the Americas. *Science* 358:1614–1617.

Van der Hammen T., Werner J., Van Dommelen H.1973. Palynological record of the upheaval of the Northern Andes: A study of the Pliocene and lower quaternary of the Colombian Eastern Cordillera and the early evolution of its high-Andean biota. *Rev. Palaeobot. Palynol*. 16:1–122.

Villagran C., Hinojosa L.F. 1997. History of the forests of southern South America. II. Phytogeographical analysis. *Rev. Chil. Hist. Nat.* 70:241–267.

Villagran C., Hinojosa L.F. 2005. Esquema biogeográfico de Chile. In: J. Llorente, J.J. Morrone, editors. *Regionalización Biogeográfica en Iberoamérica y Tópicos Afines.* México City: México, p. 551–557.

Walker J.D., Geissman J.W., Bowring S.A., Babcock L.E. 2012. Geologic Time Scale v. 4.0. Geological Society of America.

Wang S., Meyer E., McKay J.K., Matz M.V. 2012. 2b-RAD: a simple and flexible method for genome-wide genotyping. *Nat. Methods* 9:808–810.

Wiens J.J., Donoghue M.J. 2004. Historical biogeography, ecology and species richness. *Trends Ecol. Evol.* 19:639-644.

Willis J. C., H. De Vries H. B. Guppy E. M. Reid, Small J.. 1922. Age and area: a study in geographical distribution and origin of species. Cambridge University Press, Cambridge.

Winkworth R.C., Donoghue M.J. 2005. *Viburnum* phylogeny based on combined molecular data: implications for taxonomy and biogeography. *Am. J. Bot.* 92:653-666.

Zanne A.E., Tank D.C., Cornwell W.K., Eastman J.M., Smith S.A., FitzJohn R. G., Beaulieu J.M. 2014. Three keys to the radiation of angiosperms into freezing environments. *Nature* 506:89-92.

Zhang Q., Feild T.S., Antonelli A. 2015. Assessing the impact of phylogenetic incongruence on taxonomy, floral evolution, biogeographical history, and phylogenetic diversity. *Am. J. Bot.* 102:566-580.

Supplementary Figures for:

Phylogeny of *Weinmannia* (Cunoniaceae) Reveals the Contribution of the Southern Extratropics to Tropical Andean Biodiversity.

Ricardo A. Segovia*[1,2], Eduardo Aguirre-Mazzi* [3,4], Christine E. Edwards[5], Alexander G. Linan[6], Alfredo Fuentes[4,7], Andrea Chaspuengal[8], Kyle G. Dexter[9,10], Francisco Fajardo[11], William Farfan-Rios[12,13], Nora H. Oleas[8], Juan C. Penagos Zuluaga[14], J. Sebastián Tello[4]

2024-08-13

[1] *Departamento de Botánica, Universidad de Concepción, Chile*

[2] *Institute of Ecology and Biodiversity (ieb-chile.cl)*

[3] *Department of Biology, Washington University in St. Louis, St. Louis, MO, United States*

[4] *Latin America Department, Missouri Botanical Garden, St. Louis, MO, United States*

[5] *Center for Conservation and Sustainable Development, Missouri Botanical Garden, St. Louis, MO, United States*

[6] *Africa and Madagascar Program, Missouri Botanical Garden, St. Louis, MO, United States*

[7] *Herbario Nacional de Bolivia, Instituto de Ecología, Carrera de Biología, Universidad Mayor de San Andrés, La Paz, Bolivia.*

[8] *Centro de Investigación de la Biodiversidad y Cambio Climático (BioCamb) y Facultad de Ciencias del Medio Ambiente, Universidad Tecnológica Indoamérica, Machala y Sabanilla, Quito, Ecuador.*

[9] *School of GeoSciences, University of Edinburgh*

[10] *Royal Botanic Garden Edinburgh*

[11] *Botanischer Garten und Botanisches Museum Berlin-Dahlem, 14195 Berlin, Germany*

[12] *Department of Biology, Wake Forest University, Winston-Salem, NC 27106, USA.*

[13] *Andrew Sabin Center for Environment and Sustainability, Wake Forest University, Winston-Salem, NC 27106, USA.*

[14] *Research Affiliate Yale School of the Environment, Yale University. 195 Prospect Street, New Haven, CT.*

Keywords: immigration, diversification, hyperdiversity, tropics, Gondwana

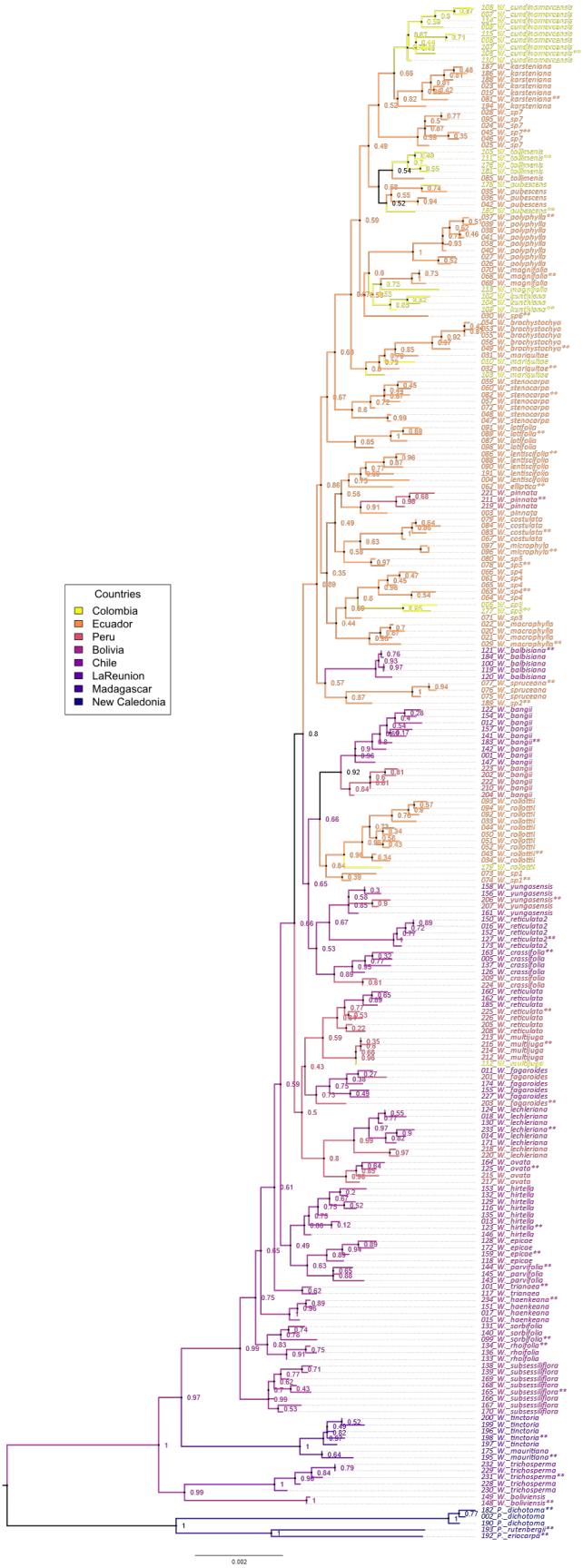
Countries
Colombia
Ecuador
Peru
Bolivia
Chile
LaReunion
Madagascar
New Caledonia
0.002

Supplementary Figure 1. Individual-level 2bRAD-seq tree for Weinmannia. Maximum Likelihood tree inferred from concatenated 2bRAD-seq data from 234 individuals of *Weinmannia* plus outgroups. Tip labels contain the Specimen_ID_code (see supplementary table 1) and Species Name. Tips labels are colored by country of origin (see legend). Bootstrap support values are shown as branch labels next to nodes. Specimens marked with ** were included in the species-level phylogenetic analyses.

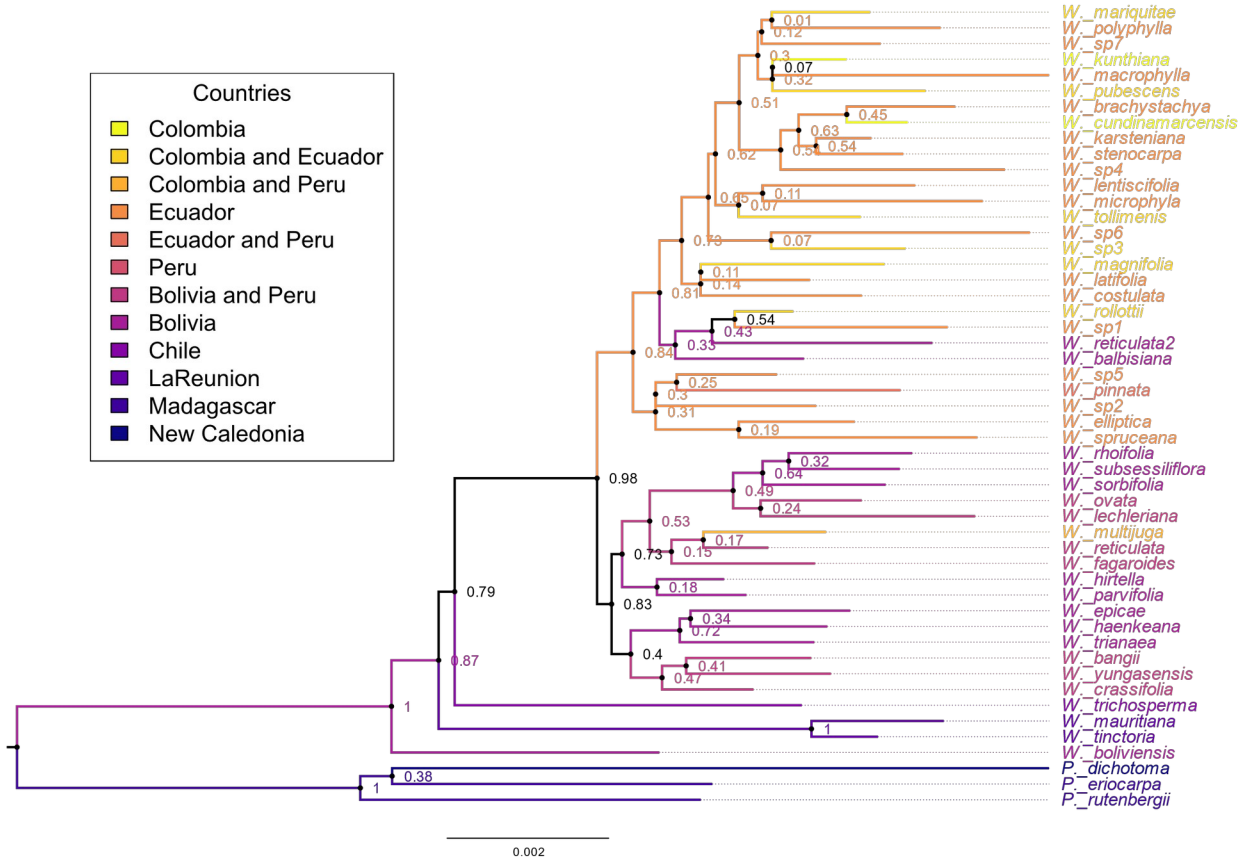

Supplementary Figure 2. Species-level Phylogeny for Weinmannia. SVDQuartets tree inferred from concatenated 2bRAD-seq data from 48 individuals of *Weinmannia* plus 3 individuals in the outgroup. Bootstrap support values are show as node labels, tip labels and branches are colored by country where species were collected. Branch labels were estimated using RAxML using this topology, (see methods).

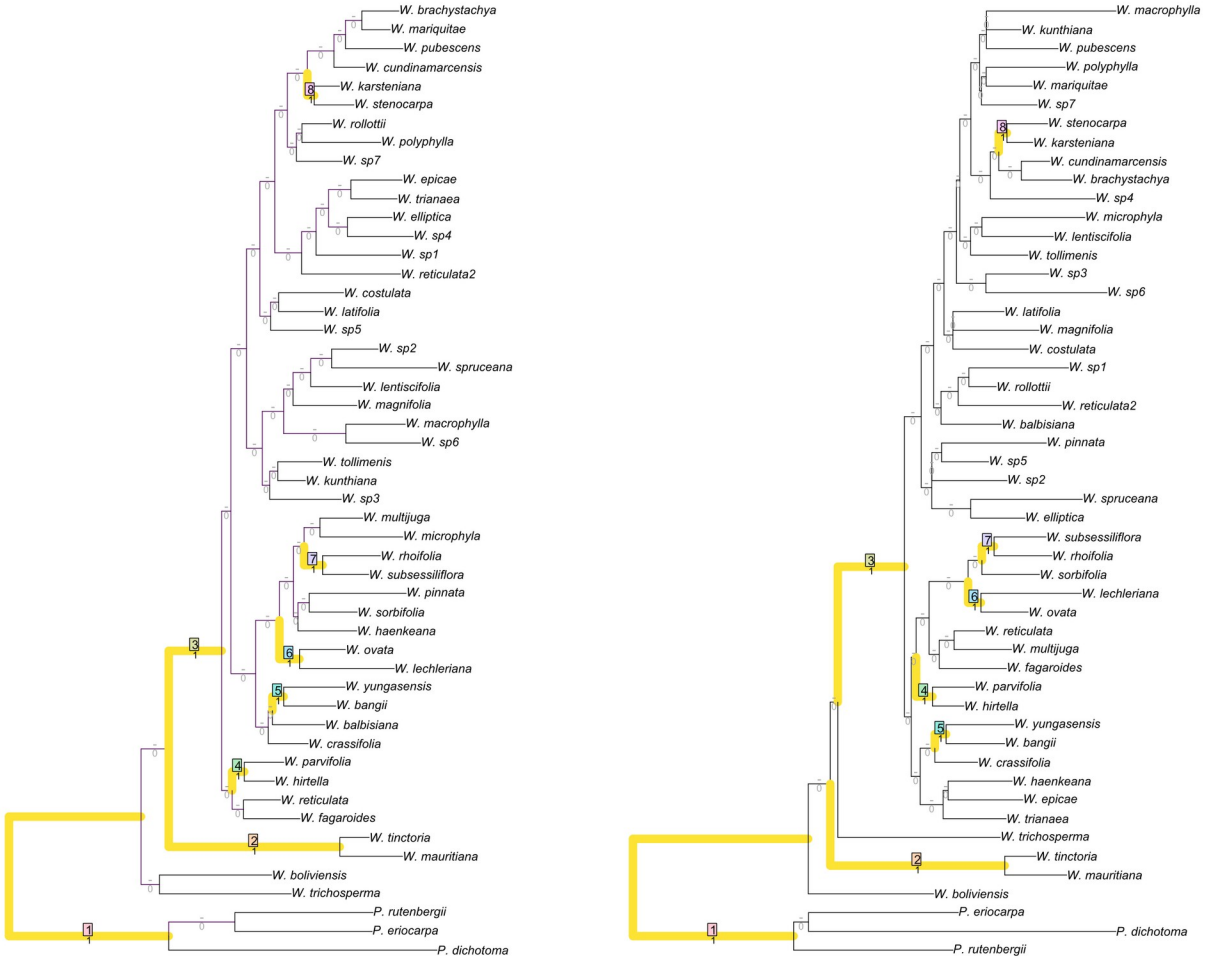

Supplementary Figure 3. Comparison of RAxML (left) and SVDQuartets (right) species-level trees. *Weinmannia* phylogeny for both methods are compared by highlighting in yellow common splitting patterns. The number of ceros depicted at the trees' nodes represent Robinson-Fould distance among both trees. (Figure generated with TreeDist Package in R)

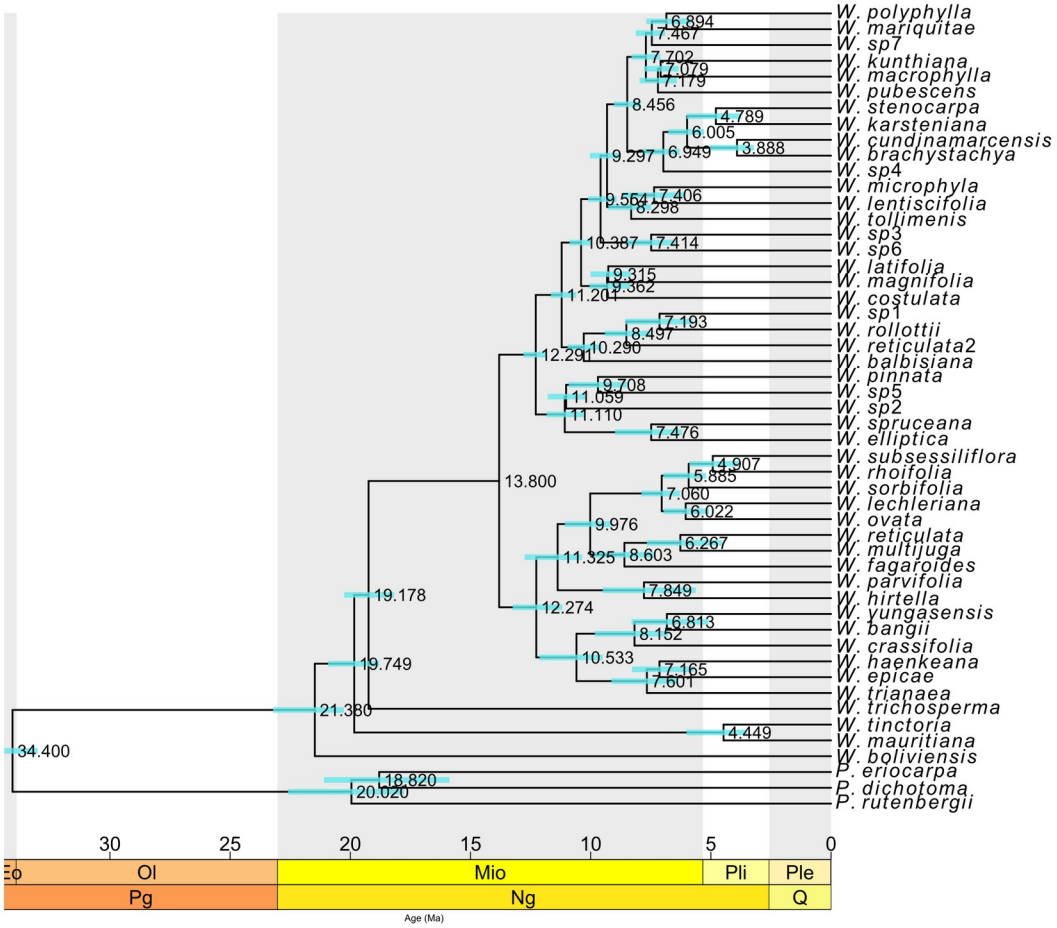

Supplementary Figure 4. SVDQuartets phylogeny with estimated divergence times of *Weinmannia* species. Median divergence age estimates across bootstrap trees with 95% confidence intervals in blue bars.

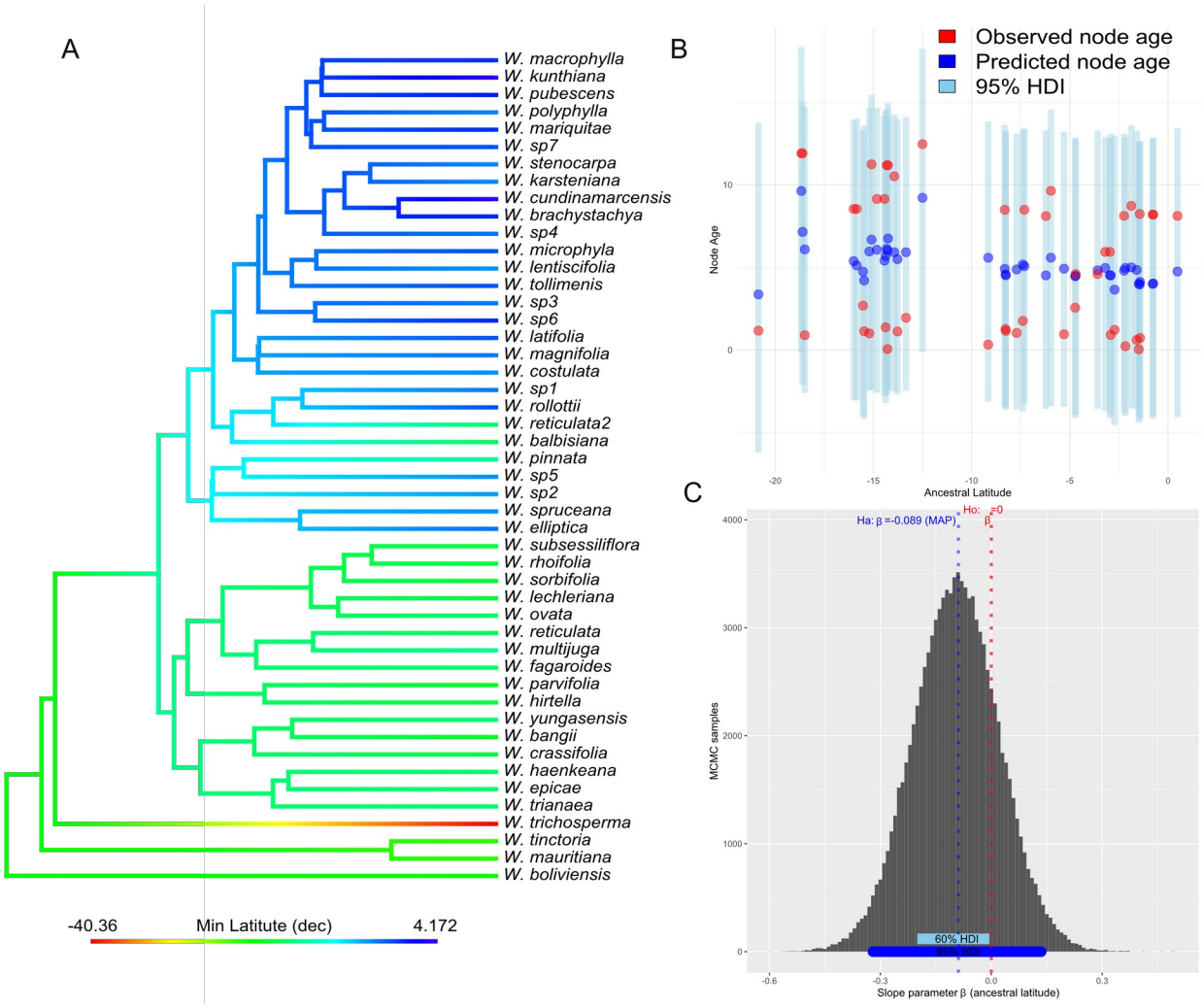

Supplementary Figure 5. Analysis for testing the dispersal from southern latitudes towards the North Andes though the Andes using topology inferred with SVDQuartets. A. Ancestral character estimate for latitude of hypothetical ancestors (nodes). Ancestral states were reconstructed on the SVDQuartets timetree using the minimum latitude of each of the 48 putative *Weinmannia* species considering reviewed accessions. The colors in the figure depict a continuous gradient of latitude, transitioning from southern temperate regions in red to northern tropical regions in blue, with intermediate latitudes in the central Andes represented in green. **B. Bayesian linear regression of node age as a function of predicted ancestral latitude: Posterior predictive check.** Observed values are represented in red dots. The blue dots represent the maximum a posteriori estimates, skyblue bars represent 95% High density intervals (HDI). **C. A posteriori probability distribution for the estimated slope coefficient for latitude as a predictor of node age.** Maximum a posteriori (MAP) is equal to β=-0.089 and the 95%HDI in blue segment goes from to -0.320 to 0.135 which includes cero. However, the 60%HDI goes from -0.196 to -0.001. This result shows the slope is different from zero (β =0) rejecting the null hypothesis with a 60% of credibility.

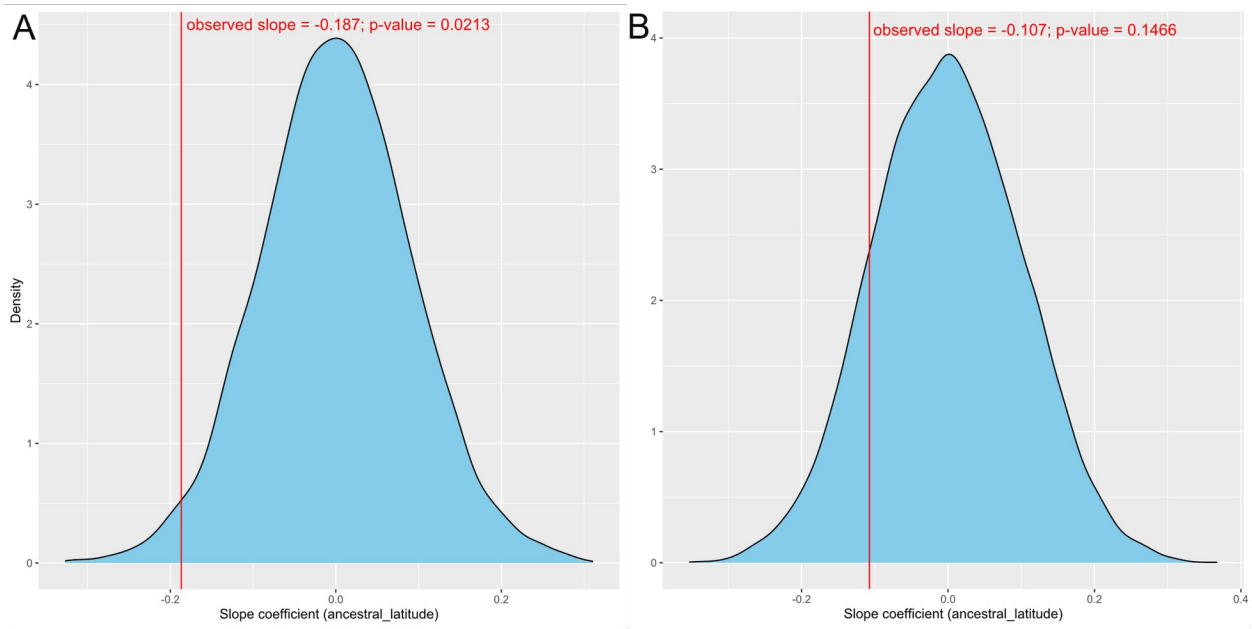

Supplementary Figure 6. Null-Hypothesis test for the slope coefficient when modelling Node Age as a function of ancestral latitude based on non-parametric bootstrap. A. Test performed using the Maximum likelihood Species-tree. Slope coefficient estimate of -0.187 was significantly different than cero p-val < 0.05 suggestin older lineages tend to be southwards. **B. Test performed using the SVDQuartet Species-tree.** In contrast with the previous estimate Slope coefficient estimate of -0.107 was not significantly different than cero p-val > 0.05 using this non-parametric bootstrap approach.